Shubnikov–de Haas measurements[25,26] have shown the complicated nature of the primary valence band by the large number of cross sections observed, and seem to confirm the existence of the second valence band, since a new cross section appears at higher carrier concentrations. However, the symmetry of this cross section does not seem to point to a {110} surface.

The nonsimple valence band, high carrier concentration ($\sim 10^{20}$ cm$^{-3}$), and high static dielectric constant of $1200\pm 200$ [27] could be responsible for the appearance of superconductivity in SnTe,[28] according to Cohen's[29] theory of superconductivity in multivalleyed degenerate semiconductors. The existence of the large number of valleys (20 valleys, if the $\sum$ maxima are taken into account) should enhance the conditions of superconductivity by providing a large number of states at the Fermi level for intervalley carrier scattering, especially since these transitions, as a consequence of large momentum transfer, are less screened than the intravalley processes. Furthermore, the transition temperature rises with increasing carrier concentration, which further supports the above conclusions.

[25] J. R. Burke, Jr., R. S. Allgaier, and B. B. Houston, Jr., Phys. Rev. Letters **14**, 360 (1965).
[26] J. R. Burke, Jr., B. B. Houston, Jr., H. T. Savage, J. Babiskin, and P. G. Siebenmann, J. Phys. Soc. Japan Suppl. **21**, 384 (1966).
[27] G. S. Pawley *et al.*, Phys. Rev. Letters **17**, 753 (1966).
[28] R. A. Hein *et al.*, in *Proceedings of the Ninth International Conference on Low-Temperature Physics, Columbus, Ohio*, edited by J. G. Daunt *et al.* (Plenum Press, Inc., New York, 1965), p. 604.
[29] M. L. Cohen, Phys. Rev. **134**, A511 (1964).

## ACKNOWLEDGMENTS

I am indebted to Professor George W. Pratt, Jr., for originally suggesting this research. Thanks are due to Dr. M. A. Gilleo and Dr. P. T. Bailey for helpful discussions. Special thanks are due to Dr. R. S. Allgaier and Dr. J. R. Burke, Jr., for extremely helpful discussions, suggestions, and for making certain unpublished results available. I am grateful to Dr. J. W. Connolly and Dr. Frank Arlinghaus for some computer programs. Acknowledgment is made of use of the computation facilities of the Management Information and Systems Department of Monsanto.

PHYSICAL REVIEW VOLUME 182, NUMBER 3 15 JUNE 1969

# Local and Nonlocal Magnetoplasma Effects in *n*-Type Lead Telluride*

S. PERKOWITZ†
*Laboratory for Research on the Structure of Matter and Physics Department, University of Pennsylvania, Philadelphia, Pennsylvania 19104*

(Received 18 November 1968)

Measurements of the derivative of the microwave absorption coefficient as a function of static magnetic field **H** have been carried out in high-mobility ($1.0\times 10^6$ cm$^2$/V sec) *n*-type lead telluride at 70 GHz and 4.2°K. The measurements were taken in the Voigt ($\mathbf{q}_0\perp\mathbf{H}$, where $\mathbf{q}_0$ is the incident radiation wave vector) and Faraday ($\mathbf{q}_0\|\mathbf{H}$) configurations, as well as in intermediate geometries, where a mixed Voigt-Faraday situation applied. The sample surface, a {110} plane, was fixed perpendicular to $\mathbf{q}_0$, and **H** was rotated in a {100} plane which contained $\mathbf{q}_0$. The data were analyzed using well-known local theory and a simplified nonlocal theory for the Azbel-Kaner and Doppler-shifted cyclotron resonances. The observed local magnetoplasma effects agreed with those predicted from the ⟨111⟩-ellipsoid model and included the hybrid resonance which has not been previously reported in lead telluride. The values deduced for the transverse mass $m_t$ and the mass ratio $K=m_l/m_t$ were $m_t/m_0=0.043\pm 0.04$ and $K=9.7\pm 1.4$ at a carrier concentration of $8.1\times 10^{17}$ cm$^{-3}$. Two weak, low-field resonances were identified as the first and second Azbel-Kaner subharmonics of a tilted-orbit cyclotron resonance. The values of the magnetic field at which the resonances and dielectric anomalies were observed in the Faraday geometry were shifted 4–19% relative to the corresponding values in the Voigt geometry, and some of these shifts agreed with the predictions of the simple Doppler-shift theory. Analysis of the Voigt dielectric-anomaly data gave a value of $10^4$ for the static part of the lattice dielectric constant. A similar value has been obtained in microwave-helicon experiments, while other methods of determination have given values near 400.

## 1. INTRODUCTION

THE free-charge carriers of a solid form a plasma which in the presence of electromagnetic radiation and a static magnetic field sustains the electromagnetic waves known as magnetoplasma modes. These modes exhibit a variety of interesting properties which depend upon the band structure of the material and the degree of nonlocality in the internal current–electric-field relation. In the limit where the current-

* Based upon a dissertation by the author submitted to the Physics Department of the University of Pennsylvania in partial fulfillment of the requirements for the Ph.D. degree. Work supported by the U. S. Office of Naval Research under Contract No. NONR 551(51) and the dissertation has been issued as Technical Report No. AD 652 620.

† Present address: General Telephone and Electronics Laboratories, Inc., Bayside, N. Y. 11360.

field relation is strictly local, the best known of the magnetoplasma effects is the cyclotron resonance, which occurs when the cyclotron frequency $\omega_c$ of the charge carriers equals the frequency $\omega$ of the applied radiation. In the spherical-mass approximation, this is the only resonance that occurs, and it appears only in the Faraday geometry, where $\mathbf{q}_0$, the wave vector of the incident radiation, is parallel to the static magnetic field $\mathbf{H}$. In the Voigt geometry with $\mathbf{q}_0 \perp \mathbf{H}$, the resonance is not seen in the ordinary mode ($\mathbf{E}_0 \| \mathbf{H}$, where $\mathbf{E}_0$ is the applied electric field), because the carrier orbit has no component which couples resonantly to the electric field, nor in the extraordinary mode ($\mathbf{E}_0 \perp \mathbf{H}$), because of screening effects due to depolarization. If the Fermi surface consists of a single ellipsoid, the cyclotron resonance appears also in the Voigt ordinary mode if $\mathbf{H}$ is not along a principal axis of the ellipsoid. Finally, if the Fermi surface consists of several ellipsoids, then the cyclotron resonance occurs in the Voigt extraordinary mode as well, together with the hybrid resonance; dielectric anomalies appear in both the Voigt and Faraday configurations.

If the current-field relationship is significantly nonlocal, two new kinds of phenomena appear in the spherical-mass approximation. In the Voigt geometry, the effect of nonlocality is to cause the resonance at $\omega=\omega_c$, as well as subharmonic resonances at $\omega=2\omega_c$, $3\omega_c$, $4\omega_c$, $\cdots$, to appear in both the ordinary and extraordinary modes. This phenomenon is called the Azbel-Kaner cyclotron resonance.[1] The second nonlocal effect, the Doppler-shifted cyclotron resonance,[2] occurs in the Faraday geometry as a change in the resonance condition from $\omega=\omega_c$ to $\omega=\omega_c-\mathbf{q}\cdot\mathbf{v}$ where $\mathbf{q}$ is the wave vector of the radiation in the medium and $\mathbf{v}$ is a characteristic electron velocity. If the Fermi surface is complicated, a complete analysis of the role of nonlocality becomes very difficult, but can be carried out to some extent in terms of the basic Azbel and Doppler-shifted cyclotron resonances.

The present work is a study of local and nonlocal magnetoplasma phenomena in lead telluride, a semiconductor which is of interest for several reasons. Its Fermi surface has been amply investigated and is simple enough to allow a theoretical treatment, yet complex enough to produce the full range of multiellipsoid effects. Its small effective mass ($\approx 0.1m_0$) and high mobility ($\approx 10^6$ cm$^2$/V sec) at liquid-helium temperatures allow the resonances to be observed at microwave frequencies and magnetic fields of a few kilogauss. Because there is no carrier freeze-out at liquid-helium temperatures, the nonlocal effects in PbTe are larger than in many other semiconductors. This property is of special interest, since almost all observations of the Azbel-Kaner and Doppler-shifted cyclotron resonances have been made in metals and semimetals.

The first magnetoplasma study of PbTe was made by Stiles *et al.*,[3] using $p$-type material at 70 GHz. In the data analysis, possible dielectric anomalies and hybrid resonances were not considered. The observed positions of the cyclotron-resonance peaks corresponded to a valence-band structure consisting of ellipsoids of revolution with their long axes along the ⟨111⟩ directions, a result which agrees with results obtained from de Haas–van Alphen[4] and Shubnikov–de Haas[5] experiments. In addition, the data included two nearly isotropic resonances which could not be explained on the basis of the ⟨111⟩-ellipsoid picture and the simplified local-cyclotron-resonance theory. Although one of these resonances occurred at about the correct field for an Azbel-Kaner subharmonic, it was not so interpreted, and no Doppler-shifted resonances were observed. In a later study, Nii[6] investigated both $n$- and $p$-PbTe at 70 GHz. His analysis included all the local multiellipsoid effects, and with the major exception of the hybrid resonance, all of these were observed. With this extended analysis, the data were completely consistent with a Fermi surface composed of ⟨111⟩ ellipsoids for both electrons and holes, and the high-field isotropic resonance observed by Stiles *et al.*, was interpreted as a dielectric anomaly which arose naturally from the ⟨111⟩ model. Nii also obtained the second, low-field, nearly isotropic resonance seen by Stiles *et al.*, and tentatively identified this as an Azbel-Kaner subharmonic. The minimum magnetic field used was not small enough to allow possible higher-order subharmonics to be detected, and no attempt was made to observe the Doppler-shifted cyclotron resonance. In a different kind of magnetoplasma experiment, Sawada *et al*,[7] studied helicons in $p$-PbTe at 70 GHz. Their results gave a value of $10^4$ for $\epsilon_s$, the static part of the lattice dielectric constant. Other measurements, including $p$-$n$ junction capacitance,[8] tunneling analysis,[9] neutron scattering,[10] and infrared reflection,[11] have all given values near 400 for $\epsilon_s$.

The aim of the present work is to examine those magnetoplasma effects which have been observed in-

[1] M. Ia. Azbel and E. A. Kaner, Zh. Eksperim. i Teor. Fiz. **30**, 811 (1956); **32**, 896 (1956) [English transls.: Soviet Phys.—JETP **3**, 772 (1956); **5**, 730 (1957)].

[2] See, e.g., P. B. Miller and R. R. Haering, Phys. Rev. **128**, 126 (1962).

[3] P. J. Stiles, E. Burstein, and D. N. Langenberg, Phys. Rev. Letters **9**, 257 (1962).

[4] P. J. Stiles, E. Burstein, and D. N. Langenberg, J. Appl. Phys. **32** (Supplement), 2174 (1961).

[5] K. F. Cuff, M. R. Ellett, and C. D. Kuglin, J. Appl. Phys. **32** (Supplement), 2179 (1961).

[6] R. Nii, J. Phys. Soc. Japan **19**, 58 (1964).

[7] Y. Sawada, E. Burstein, D. L. Carter, and L. Testardi, in *Proceedings of the Symposium on Plasma Effects in Solids, Paris, 1964*, edited by J. Bok (Academic Press Inc., New York, 1965), p. 71.

[8] Y. Kanai and K. Shohno, Japan. J. Appl. Phys. **2**, 6 (1963).

[9] H. M. Day and A. C. Macpherson, Proc. IEEE **51**, 1362 (1963).

[10] W. Cochran, Phys. Letters **13**, 193 (1964).

[11] E. G. Bylander and M. Hass, Solid State Commun. **4**, 51 (1966).

conclusively or not at all in the previous investigations; these are the hybrid resonance and both nonlocal resonances. It is also of value to remeasure $\epsilon_s$ by a method other than that used by Sawada *et al.*, and the determination is made here from dielectric-anomaly data.

## 2. LOCAL MAGNETOPLASMA THEORY

The magnetoplasma-radiation interaction is characterized by $\sigma$, the conductivity tensor of the medium. This quantity can be obtained from the equations of motion for the free carriers, provided the form of the mass tensor is known. The accepted picture of the Fermi surface in PbTe is shown in Fig. 1. Each of the ellipsoids is conveniently described by the parameters $K=m_l/m_t$ and $m_t$, where $m_l$ and $m_t$ are the mass-tensor components parallel and transverse, respectively, to the $\langle 111\rangle$ directions.

In CGS units (which will be used throughout) the equation of motion for the carriers in the $k$th ellipsoid is

$$\mathbf{m}_k\cdot\left(\frac{d\mathbf{v}_k}{dt}+\frac{\mathbf{v}_k}{\tau}\right)=e\left(\mathbf{E}+\frac{\mathbf{v}_k\times\mathbf{H}}{c}\right), \tag{1}$$

where $\mathbf{m}_k$ is the mass tensor, $\mathbf{v}_k$ is the drift velocity, $\tau$ is the scattering time (assumed constant and isotropic), $e$ is the carrier charge, $\mathbf{E}$ is the self-consistent internal microwave electric field, $\mathbf{H}$ is the static magnetic field, and $c$ is the velocity of light. In the local limit, $\mathbf{E}$ is independent of position and is taken as $\mathbf{E}\propto e^{i\omega t}$. In this case, Eq. (1) can be solved immediately for $\mathbf{v}_k$; then, using the definitions

$$\mathbf{J}=\tfrac{1}{4}ne\sum_{k=1}^{4}\mathbf{v}_k=\boldsymbol{\sigma}\cdot\mathbf{E}, \tag{2}$$

where $\mathbf{J}$ is the internal current density and $n$ is the total carrier concentration, $\boldsymbol{\sigma}$ may be obtained.

The electromagnetic response of the medium is obtained by inserting $\boldsymbol{\sigma}$ into Maxwell's equations. The

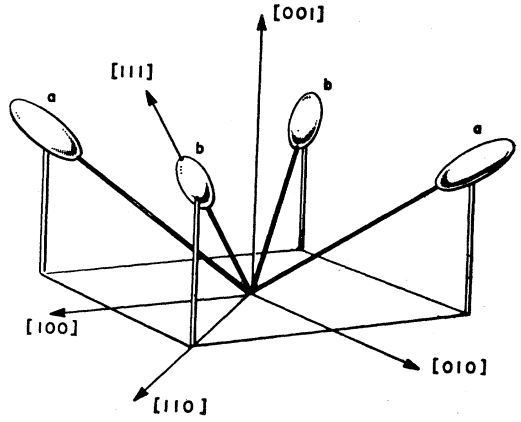


FIG. 1. Fermi surface of lead telluride.

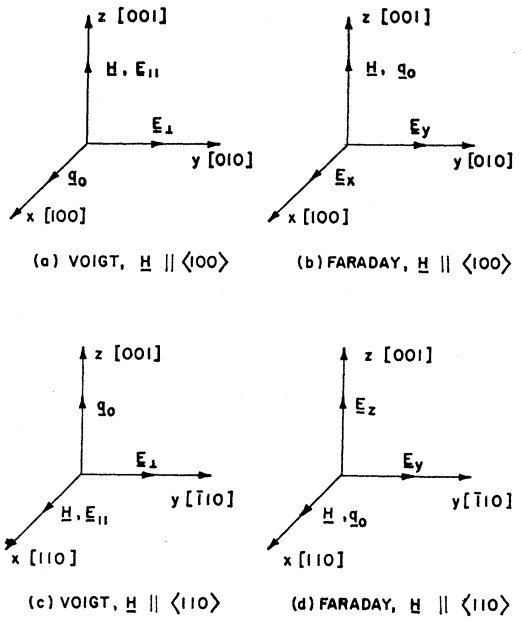


FIG. 2. Coordinate systems used in the calculations.

quantity of interest is the complex index of refraction $\eta$, defined by

$$\eta=q/q_0, \tag{3}$$

where $\mathbf{q}$ and $\mathbf{q}_0$ are the internal and external wave vectors, respectively. $\eta^2$ is calculated from the dispersion relation

$$q^2\mathbf{E}-\mathbf{q}(\mathbf{q}\cdot\mathbf{E})=q_0^2\boldsymbol{\varepsilon}\cdot\mathbf{E}, \tag{4}$$

which has been written in the form suitable for plane waves, and where the effective dielectric tensor $\boldsymbol{\varepsilon}$ is defined by

$$\boldsymbol{\varepsilon}=\epsilon_L\mathbf{I}+4\pi\boldsymbol{\sigma}/i\omega. \tag{5}$$

Here, $\epsilon_L$ is the lattice dielectric constant of the medium and $\mathbf{I}$ is the unit tensor. The experimentally measured quantity is related to the power absorption coefficient $A$ which is given by

$$A=4\,\mathrm{Re}\eta/|\eta+1|^2. \tag{6}$$

Nii[6] and Numata and Uemura[12] have calculated $\eta^2$ and $A$ for PbTe in the Voigt geometry, with $\mathbf{H}$ in a {100} plane; they have paid particular attention to the high-symmetry directions $\mathbf{H}\|\langle 100\rangle$ and $\mathbf{H}\|\langle 110\rangle$. Their results (and notation) will be used here and extended to include the Faraday geometry with $\mathbf{H}\|\langle 100\rangle$ and $\mathbf{H}\|\langle 110\rangle$. The coordinate systems used in the calculations are shown in Fig. 2, where specific crystal directions have been chosen for definiteness. The figure also illustrates the Voigt and Faraday geometries.

In all the results which follow, the approximation $\omega\tau\to\infty$ has been made. This approximation simplifies the algebra considerably and is reasonable since the

[12] H. Numata and Y. Uemura, J. Phys. Soc. Japan 19, 2140 (1964).

experimental value of $\omega\tau$ is large. The positions of resonances will be given accurately, but the line shapes near resonance cannot be determined.

For the case with highest symmetry, $\mathbf{H}\|\langle 100\rangle$, the result for the effective dielectric tensor is

$$\varepsilon\langle 100\rangle=\begin{bmatrix}\epsilon_{xx} & \epsilon_{xy} & 0\\ -\epsilon_{xy} & \epsilon_{xx} & 0\\ 0 & 0 & \epsilon_{zz}\end{bmatrix}, \tag{7}$$

where

$$\begin{aligned}\epsilon_{xx}&=\epsilon_L-\omega_{p11}^2/\Delta_{11},\\ \epsilon_{xy}&=i(\omega_{p12}^2/\Delta_{11})\omega_{c11}/\omega,\\ \epsilon_{zz}&=\epsilon_L-(\omega_{p11}^2/\omega^2)(\omega^2-\omega_{c33}^2)/\Delta_{11}.\end{aligned} \tag{8}$$

Defining $\omega_{ct}=|e|H/cm_t$ and $\omega_{pt}^2=4\pi ne^2/m_t$, the parameters in Eq. (8) are

$$\begin{aligned}&\omega_{c11}=\omega_{ct}\left(\frac{K+2}{3K}\right)^{1/2}, \quad \omega_{p11}^2=\omega_{pt}^2\left(\frac{2K+1}{3K}\right),\\ &\omega_{c33}=\omega_{ct}\left(\frac{3}{2K+1}\right)^{1/2}, \quad \omega_{p12}^2=\omega_{pt}^2\left(\frac{K+2}{3K}\right)^{1/2},\\ &\Delta_{11}=\omega^2-\omega_{c11}^2.\end{aligned} \tag{9}$$

The quantities $\omega_{c11}$ and $\omega_{c33}$ are cyclotron frequencies, and $\omega_{p11}$ and $\omega_{p12}$ are plasma frequencies. From Eq. (7) and the dispersion relation, the refractive indices for the Voigt extraordinary, Voigt ordinary, and Faraday

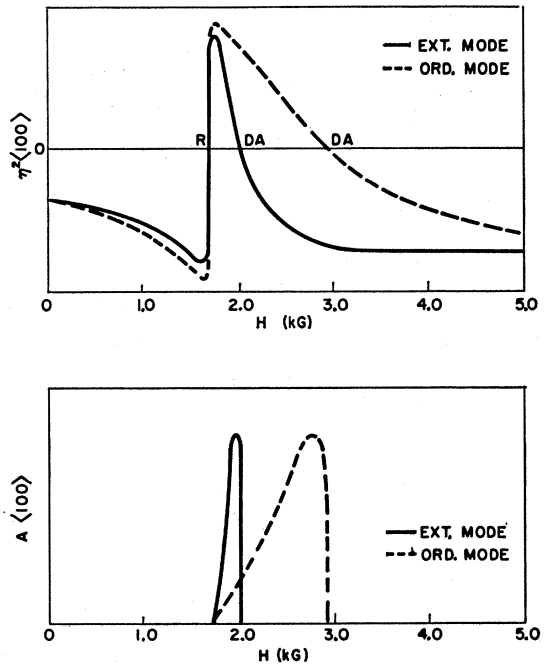


FIG. 3. Schematic plot of $\eta^2$ and $A$ as a function of magnetic field for the Voigt ordinary and extraordinary modes with $\mathbf{H}\|\langle 100\rangle$. R = resonance; DA = dielectric anomaly.

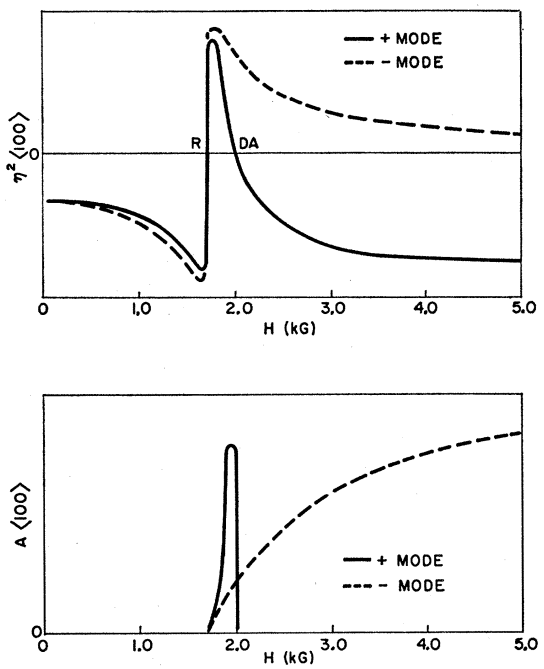


FIG. 4. Schematic plot of $\eta^2$ and $A$ as a function of magnetic field for the Faraday (+) and (−) modes with $\mathbf{H}\|\langle 100\rangle$.

cases are found to be

$$\begin{aligned}\eta_e^2\langle 100\rangle&=\epsilon_{xx}+\epsilon_{xy}^2/\epsilon_{xx},\\ \eta_o^2\langle 100\rangle&=\epsilon_{zz},\\ \eta_\pm^2\langle 100\rangle&=\epsilon_{xx}\pm i\epsilon_{xy},\end{aligned} \tag{10}$$

where $\eta_\pm^2$ refers to the two possible Faraday modes. These refractive indices and the associated absorption coefficients are schematically plotted against $H$ in Figs. 3 and 4, where the values $K=10$, $m_t/m_0=0.05$, $\epsilon_L=400$ (which is the approximate value of $\epsilon_L$ taking $\epsilon_s=400$ and $\omega=2\pi\times 70$ GHz), and $\omega=2\pi\times 70$ GHz have been used. The main features of these plots can be interpreted as follows.

*1. Tilted-orbit cyclotron resonance.* The resonance at 1.8 kG in the Voigt ordinary mode occurs at $\omega=\omega_{c11}$. The resonance appears because $\mathbf{H}$ does not lie along any principal axis of the mass ellipsoids; as a result, the electron orbits in real space are tilted relative to the plane perpendicular to $\mathbf{H}$ and have a component which couples resonantly to $\mathbf{E}$. Since all four ellipsoids are tilted symmetrically relative to $\mathbf{H}$, only the single resonance at $\omega=\omega_{c11}$ occurs. The possibility of the tilted-orbit effect was first pointed out by Smith, Hebel, and Buchsbaum (SHB) and observed by them in bismuth.[13]

*2. Incompletely screened cyclotron resonance.* SHB have shown that, if two or more mass ellipsoids exist, the net longitudinal field cannot be large enough to screen out the resonance completely, and this is the reason that

[13] G. E. Smith, L. C. Hebel, and S. J. Buchsbaum, Phys. Rev. 129, 154 (1963).

the resonance at $\omega=\omega_{c11}$ appears in the Voigt extraordinary mode. In that geometry, the electron orbits are left-handed ellipses in the $x\,y$ plane with eccentricity

$$\epsilon_{\text{orbit}}=[(2K+1)/(K+2)]^{1/2}, \tag{11}$$

while the internal fields at $\omega=\omega_{c11}$ are elliptically polarized in the right-hand sense with eccentricity

$$\epsilon_{\text{field}}=\frac{\omega_{p12}^2}{\omega_{p11}^2}=\frac{[3K(K+2)]^{1/2}}{2K+1}. \tag{12}$$

The difference in ellipticities ensures that there is a component of $\mathbf{E}$ which can couple to the electrons. For $K=10$, this coupling is only 14% of the coupling that would exist if there were no screening effects at all, so that the resonance at $\omega=\omega_{c11}$ is still heavily screened and may be expected to appear weakly.

*3. Dielectric anomaly.* In both Voigt modes, and in the Faraday (+) mode, there are points where the index of refraction becomes zero. Such points have been called dielectric anomalies by Boyle *et al.*[14] In the absorption coefficient, these anomalies appear as sharp drops in absorption to zero. The dielectric anomalies are of particular importance in PbTe because, unlike the cyclotron resonances, their position in magnetic field depends upon the value of the lattice dielectric constant $\epsilon_L$. This dependence arises from the fact that the condition $\eta^2=0$ can always be put in the form

$$\epsilon_L/n=f, \tag{13}$$

where the carrier concentration $n$ comes from plasma frequency terms, and $f$ is the appropriate function of $H$, $\omega$, $K$, and $m_t$. Thus, $\epsilon_L$ can be determined from the position in magnetic field of the dielectric anomaly if all the other parameters are known.

For the second high-symmetry direction $\mathbf{H}\|\langle 110\rangle$, there are two nonequivalent pairs of ellipsoids, denoted by $a$ and $b$ in Fig. 1. Correspondingly, two different cyclotron frequencies appear in the refractive indices. The effective dielectric tensor is

$$\boldsymbol{\epsilon}\langle 110\rangle=\begin{bmatrix}\epsilon_{xx} & 0 & 0\\ 0 & \epsilon_{yy} & \epsilon_{yz}\\ 0 & -\epsilon_{yz} & \epsilon_{zz}\end{bmatrix}, \tag{14}$$

where

$$\begin{aligned}
\epsilon_{xx}&=\epsilon_L-\frac{\omega_{pt}^2}{2\omega^2}\left(1+\frac{K+2}{3K}\frac{\Delta_{11}}{\Delta_b}\right),\\
\epsilon_{yy}&=\epsilon_L-\left(\frac{\omega_{pa22}^2}{\Delta_a}+\frac{\omega_{pb22}^2}{\Delta_b}\right),\\
\epsilon_{zz}&=\epsilon_L-\omega_{pa33}^2[(\Delta_a)^{-1}+(\Delta_b)^{-1}],\\
\epsilon_{yz}&=i\left(\frac{\omega_{pa23}^2}{\Delta_a}\frac{\omega_{ca}}{\omega}+\frac{\omega_{pb23}^2}{\Delta_b}\frac{\omega_{cb}}{\omega}\right),\\
\Delta_a&=\omega^2-\omega_{ca}^2,\\
\Delta_b&=\omega^2-\omega_{cb}^2.
\end{aligned} \tag{15}$$

[14] W. S. Boyle, A. D. Brailsford, and J. K. Galt, Phys. Rev. **109**, 1396 (1958).

The two cyclotron frequencies and the plasma frequency $\omega_{pa33}$ are defined by

$$\begin{aligned}
\omega_{ca}&=\omega_{ct}K^{-1/2},\\
\omega_{cb}&=\omega_{ct}[(2K+1)/3K]^{1/2},\\
\omega_{pa33}^2&=\tfrac{1}{2}\omega_{pt}^2(2K+1)/3K.
\end{aligned} \tag{16}$$

The remaining parameters in Eq. (15) are not of immediate interest and are given by Nii. The refractive indices obtained from the dispersion relation are

$$\begin{aligned}
\eta_e^2\langle 110\rangle&=\epsilon_{yy}+\epsilon_{yz}^2/\epsilon_{zz},\\
\eta_o^2\langle 110\rangle&=\epsilon_{xx},\\
\eta_\pm^2\langle 110\rangle&=\tfrac{1}{2}\{(\epsilon_{yy}+\epsilon_{zz})\pm[(\epsilon_{yy}-\epsilon_{zz})^2-4\epsilon_{yz}^2]^{1/2}\}.
\end{aligned} \tag{17}$$

The behavior of these functions can be described briefly. $\eta_e^2$ and $\eta_o^2$ each exhibit a cyclotron resonance, with the extraordinary-mode resonance at $\omega=\omega_{ca}$ and the ordinary-mode resonance at $\omega=\omega_{cb}$. The former represents an incompletely screened cyclotron resonance and the latter a tilted-orbit resonance. The extraordinary mode also exhibits a new kind of resonance which did not appear for $\mathbf{H}\|\langle 100\rangle$. This is the hybrid resonance, which has been discussed by SHB. In the present case, it arises from the longitudinal field coupling between electrons in the $a$ and $b$ ellipsoid pairs. The condition for the hybrid resonance is $\epsilon_{zz}=0$; that is, it occurs at the value of $H$ satisfying

$$2\omega^2-(\omega_{ca}^2+\omega_{cb}^2)=(Q/\omega^2)(\omega^2-\omega_{ca}^2)(\omega^2-\omega_{cb}^2), \tag{18}$$

where $Q=\epsilon_L\omega^2/\omega_{pa33}^2\propto\epsilon_L/n$. Thus the position of the hybrid resonance depends upon $\epsilon_L/n$, but turns out to be insensitive to the value of this ratio. For typical values of the parameters, $Q$ is small and the position of the hybrid resonance is given approximately by

$$\omega=\tfrac{1}{2}(\omega_{ca}^2+\omega_{cb}^2)^{1/2}. \tag{19}$$

In addition to the resonances, dielectric anomalies appear in both Voigt modes. The ordinary-mode dielectric anomaly is separated from the resonance at $\omega=\omega_{cb}$ by less than 0.2 kG. Dielectric anomalies and the resonances at $\omega=\omega_{ca}$ and $\omega=\omega_{cb}$ also appear in the Faraday modes, but the hybrid resonance does not, because there is no longitudinal field in the Faraday geometry.

One other aspect of the magnetoplasma effects in PbTe remains to be discussed, namely, the state of polarization of the Faraday modes. In the spherical-mass approximation, the two Faraday modes are circularly polarized in opposite senses. In PbTe, for $\mathbf{H}\|\langle 100\rangle$, the same result holds, because each ellipsoid has the same circular cross section in the plane perpendicular to $\mathbf{H}$. For $\mathbf{H}\|\langle 110\rangle$, however, the $a$ and $b$ ellipsoids present different cross sections, and the two Faraday modes are elliptically polarized. Therefore, for either linearly or circularly polarized exciting radiation, single-mode excitation cannot be obtained in the sample. This fact will be important in the discussion of the Doppler-shifted cyclotron resonance.

### 3. NONLOCAL MAGNETOPLASMA THEORY

No complete theory exists for nonlocal effects in a multiellipsoid semiconductor. Suzuki *et al.*[15] have considered nonlocal effects in the Voigt geometry for a Fermi surface composed of a single ellipsoid, but have not extended the theory to the multiellipsoid case. Their starting point was the Boltzmann equation, and their results appear in a complex form that is not suited for giving simple physical insights into nonlocality. When the nonlocal effects are small, as is the case here, matters are simplified by bypassing the full Boltzmann equation and starting instead from the usual equations of motion. Hebel[16] has used this approach to treat weak Azbel-Kaner cyclotron resonance in the Voigt ordinary mode, and has applied the results to bismuth for the case where $\mathbf{H}$ lies along the major axis of a mass ellipsoid. In connection with the present work, a similar method has been developed and extended to include the Voigt extraordinary and Faraday configurations. The details of the calculation will be given elsewhere. Only the results will be used here to give a semiquantitative understanding of nonlocal phenomena in PbTe.

The nonlocal equations of motion are obtained by introducing a spatially dependent $\mathbf{E}$ and $\mathbf{v}$ into Eq. (1) and Fourier-transforming in space to yield

$$m\left[\frac{\partial \mathbf{v}(q,t)}{\partial t}+\left(\frac{1}{\tau}-iqv_q\right)\mathbf{v}(q,t)\right] = e\left(\mathbf{E}(q)e^{i\omega t}+\frac{\mathbf{v}(q,t)\times\mathbf{H}}{c}\right) \quad (20)$$

in the spherical-mass approximation. Here, $v_q$ is the component of electron velocity parallel to the direction of propagation of the radiation, and the transformed velocity and field are defined by

$$\mathbf{v}(q,t)=\int_0^\infty \mathbf{v}(s,t)e^{iqs}ds \text{ and } \mathbf{E}(q)=\int_0^\infty \mathbf{E}(s)e^{iqs}ds, \quad (21)$$

where $s$ is the component of electron position parallel to the propagation direction. To solve Eq. (20) it is first necessary to determine $v_q$. It is found that this longitudinal velocity is independent of time in the Faraday geometry, but is proportional to $e^{i\omega_c t}$, where $\omega_c$ is the cyclotron frequency $|e|H/mc$, in the Voigt geometry. As an immediate consequence of the fact that $v_q$ can take these two forms, two distinct types of nonlocal effect exist. In the Faraday geometry, the nonlocal contribution can be expanded in powers of $qv_F/\omega$, where $v_F$ is the Fermi velocity. To order $(qv_F/\omega)^2$, the effect of the nonlocal terms is to shift the position of the cyclotron resonance from $\omega_c/\omega=1$ to

$$\omega_c/\omega=1+\rho^{1/3}, \quad (22)$$

where $\rho=\frac{1}{5}(v_F^2\omega_p^2/c^2\omega^2)$ and $\omega_p^2=4\pi ne^2/m$ is the plasma frequency. The cyclotron resonance is said to be "Doppler-shifted" to a higher magnetic field. In the Voigt arrangement, for both modes, the parameter of nonlocality is $qv_F/\omega_c$. Here, the nonlocal terms produce the Azbel-Kaner subharmonics which appear at $\omega=p\omega_c$ and have strengths proportional to $(qv_F/\omega_c)^{2p}$, where $p=2, 3, 4, \cdots$. The expansions in powers of $qv_F/\omega$ and $qv_F/\omega_c$ are valid only if these quantities are less than unity. This is generally the case in semiconductors at microwave frequencies. For $n$-type PbTe with $n\approx 10^{18}$ cm$^{-3}$, $qv_F/\omega$ is about 0.5 and $qv_F/\omega_c$ is 0.5 or less at 70 GHz.

By using the appropriate mass tensors, Eq. (20) can be used to describe nonlocal behavior in PbTe. The most interesting phenomena are obtained for $\mathbf{H}\|\langle 110\rangle$ where, in the Voigt geometry, Azbel-Kaner subharmonics can appear at both $\omega=p\omega_{ca}$ and $\omega=p\omega_{cb}$. The strengths of both the $a$ and $b$ subharmonics decrease very rapidly as $p$ increases, but the $b$ subharmonics are $(\omega_{ca}/\omega_{cb})^{2p}\approx(3)^{2p}$ times as strong as the $a$ subharmonics. In the Faraday geometry, the longitudinal velicity $v_q$ for the $a$ ellipsoids is independent of time and a Doppler-shifted resonance like that given by Eq. (22) results. For the tilted $b$ pair, $v_q$ contains both a constant term and a time-dependent term. This form for $v_q$ suggests that the resonance at $\omega=\omega_{cb}$ will both undergo a Doppler shift and generate subharmonics, but the theory is not adequate to determine whether the subharmonics themselves are shifted.

This discussion has shown that the Doppler-shifted resonances should occur, but that the magnitudes of the shifts cannot be obtained without going through the complete solution of the anisotropic, nonlocal equations of motion. A simpler method can be used, which derives from the fact that the moving electron actually sees a Doppler-shifted frequency $\omega+qv_q$ so that the cyclotron resonance occurs at

$$\omega_c=\omega+qv_q. \quad (23)$$

By taking $q=q_0\eta_\pm$, where $\eta_\pm$ is the local Faraday index of refraction, and taking an appropriate average of $v_q$ over the Fermi surface, Eq. (23) can be put in the form of Eq. (22). This procedure can be generalized to the case at hand, with Eq. (23) written as

$$[(\omega_{ci}/\omega)-1]^2=(\bar{v}_{Fi}/c)^2\eta_\pm^2\langle 110\rangle, \quad (24)$$

where the subscript represents the $a$ or $b$ ellipsoids, $\bar{v}_{Fi}$ is the average of $v_{qi}$ over the Fermi surface, and $\eta_\pm^2\langle 110\rangle$ is defined by Eq. (17). The left side of Eq. (24) is a parabola centered at the position of local resonance $\omega=\omega_{ci}$. Both sides of the equation can be plotted as functions of $H$, and the point of intersection of the two curves represents the position of the Doppler-shifted resonance. Such a plot, using $\eta_+^2\langle 110\rangle$ only, is shown

[15] H. Suzuki, M. Hattori, and K. Ariyama, J. Phys. Soc. Japan **16**, 1947 (1961).
[16] L. C. Hebel, Phys. Rev. **138**, A1641 (1965).

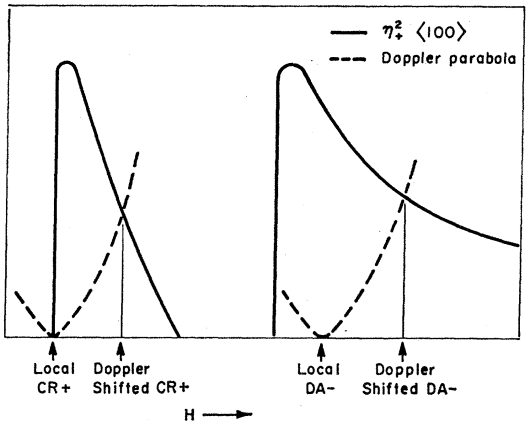


FIG. 5. Graphical solution for the positions of Doppler-shifted phenomena.

schematically in Fig. 5. Included in the plot is a Doppler parabola which is centered at a dielectric anomaly appearing in the (−) mode. This parabola would not intersect $\eta_-^2\langle 110\rangle$ anywhere except at its origin, indicating that the dielectric anomaly is not Doppler-shifted. This result is certainly correct since, by definition, the right side of Eq. (24) is zero at a dielectric anomaly. However, as the figure shows, the parabola does intersect $\eta_+^2\langle 110\rangle$, and the question arises whether this solution has any physical meaning. In the present case, because of the lack of single-mode excitation for $\mathbf{H}\|\langle 110\rangle$, it appears that this sort of "cross-mode" effect can exist and a Doppler-shifted dielectric anomaly can occur.

## 4. EXPERIMENTAL METHODS

The experiments were carried out at 70 GHz and 4.2°K using a sample of single-crystal $n$-type PbTe. At 4.2°K, Hall data gave a carrier concentration of $8.1\times10^{17}$ cm$^{-3}$ and a mobility of $1.0\times10^6$ cm$^2$/V sec. This high mobility, which corresponds to an $\omega\tau$ of 25 at 70 GHz, was obtained by annealing the sample in a tellurium atmosphere. The annealing procedure has been described by Sato *et al.*[17] The sample was cut in the form of a rectangular parallelopiped approximately $7\times6\times1$ mm thick and was electropolished to produce smooth, flat surfaces. All the faces of the sample were {110} planes to within 1° as determined by x-ray diffraction. It would have been preferable to use a sample with {100} faces because of the simpler symmetry, but attempts at annealing such samples failed.

The experiments were carried out with a standard microwave spectrometer operating at 70 GHz. The usual field modulation and lock-in detection system was used and the data consisted of recorder traces of $dA/dH$ versus $H$. A technique for obtaining $d^2A/dH^2$ was found to be useful in examining very weak effects. The sample was mounted as one wall of a high-$Q$ cylindrical cavity which resonated in a $TE_{111}$ mode. A mode-splitting pin was used to separate the degenerate cavity mode into two orthogonal modes of different frequency. In both of these modes, the major part of the microwave electric field lay in a given direction (either parallel or perpendicular to the splitting pin) but about 15% of the absorbed power came from other components of the field, so that some mode-mixing effects might be expected. The sample was mounted so that the field in the more strongly excited of the two modes was along a ⟨100⟩ direction, $\mathbf{H}$ lay in the corresponding {100} plane, and $\mathbf{q}_0$ was along a ⟨110⟩ direction in the same {100} plane. The {100} plane was located to within 2° by a preliminary cyclotron-resonance experiment. Since $\mathbf{H}$ was free to rotate in the {100} plane, this arrangement made it possible to turn $\mathbf{H}$ from a ⟨110⟩ direction along $\mathbf{q}_0$ to a new ⟨110⟩ direction perpendicular to $\mathbf{q}_0$, that is, from the Faraday configuration to the Voigt configuration.

## 5. EXPERIMENTAL RESULTS AND DATA ANALYSIS

The primary experimental results are shown in Fig. 6, where the results are plotted against $\theta$, the angle between $\mathbf{H}$ in a {100} plane and a ⟨100⟩ direction. The $[01\bar{1}]$ direction in the figure is along the incident wave vector, so that the angles $\theta=45°$ and $\theta=135°$ represent the Voigt and Faraday configurations, respectively. The points in the figure were obtained from experimental traces like that shown in Fig. 7 by plotting against $\theta$ the values of $H$ for all the maximum and minimum points of the traces, and then taking the means between paired maxima and minima. The theoretical curves in Fig. 6 were obtained from the calculations of Numata and Uemura for the Voigt geometry, and therefore are strictly valid only near $\theta=45°$. The theoretical curve for the ordinary-mode dielectric anomaly (ODA) has been omitted for clarity. The broken curve labeled ABC has been drawn as a smooth fit to the experimental points which lie between the theoretical hybrid resonance and ordinary-mode resonance curves near $\theta=45°$. Though the data were taken using only the cavity mode which would correspond to the extraordinary mode at $\theta=45°$, it is apparent that mode-mixing occurs, since an ordinary-mode effect also appears.

The first step in the analysis is to obtain values for the mass parameters $K$ and $m_t$. To prevent possible Doppler effects from playing a spurious role in the determination of these quantities, they have been calculated from the data at $\theta=45°$. At this angle, the point at 3.4 kG represents the extraordinary-mode resonance (ER) at $\omega=\omega_{ca}$, and the 1.3 kG point is taken as the ordinary-mode resonance (OR) at $\omega=\omega_{cb}$. From these results, the values $K=9.7\pm1.4$ and $m_t/m_0=0.043\pm0.04$ are obtained. The theoretical ER and OR curves use

[17] Y. Sato, M. Fujimoto, and A. Kobayashi, Japan J. Appl. Phys. 2, 688 (1963).

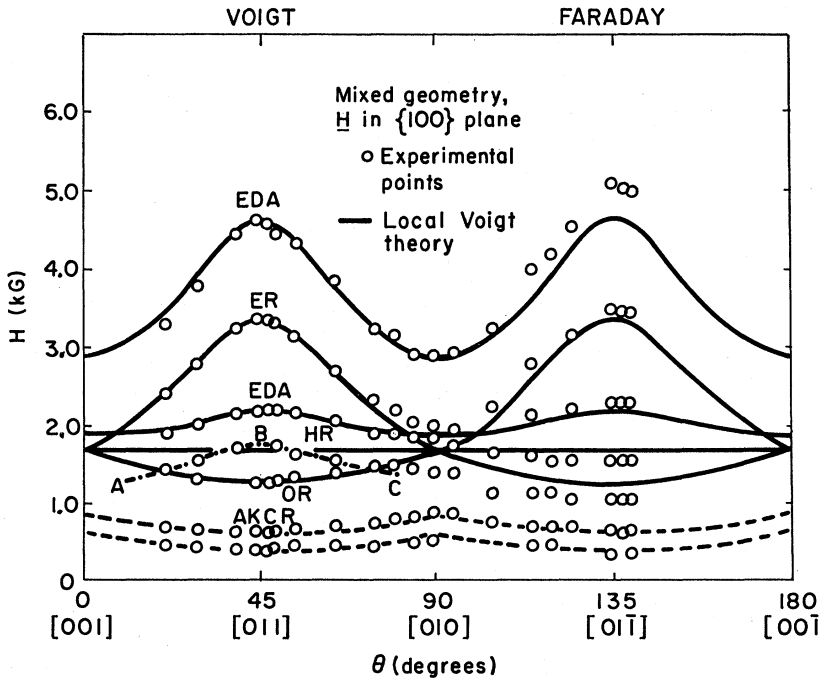


FIG. 6. Experimental results and theoretical fit for the positions of resonances and dielectric anomalies as a function of $\theta$, the angle between **H** and a ⟨100⟩ direction, in $n$-type PbTe. R = resonance, DA = dielectric anomaly, HR = hybrid resonance, E = extraordinary mode, O = ordinary mode, and AKCR = Azbel-Kaner cyclotron resonance.

these values and are seen to fit the data quite well up to $\theta = 90°$.

The choice of the 1.3-kG line as the OR and not the nearby ODA is based on two considerations. First, this choice gives a better fit to the low-field lines near 0.65 and 0.45 kG, which are interpreted as the first and second Azbel-Kaner subharmonics of the OR. Also, this choice is consistent with the interpretation of the curve ABC in the figure as the hybrid resonance (HR). This discussion does not necessarily mean that the ODA does not appear at all. It is possible that it appears more weakly than the OR and cannot be easily resolved because the two effects are very close in magnetic field.

Figure 8 is an expanded view of the experimental curve ABC, together with two theoretical curves for the HR in the Voigt geometry. Both of the latter are derived from the condition $\epsilon_{zz} = 0$, and it will be recalled that the position of the HR depends upon $K$, $m_t$, and $Q \propto \epsilon_L/n$. The flat curve is calculated for the values of $K$ and $m_t$ obtained above and $Q = 0$; the predicted position for the HR is then 1.70 kG. It is seen that the peak of ABC is shifted up a few percent from this value. The second theoretical curve is drawn for the same values of $K$ and $m_t$, $n = n_{\text{Hall}} = 8.1 \times 10^{17}$ cm$^{-3}$, and $\epsilon_L = 10^4$, which yield $Q = 0.1$. This value of $Q$ gives an upward shift of about 2% in the predicted position of the HR at $\theta = 45°$, while the shift for $\epsilon_L = 400$ would be less than

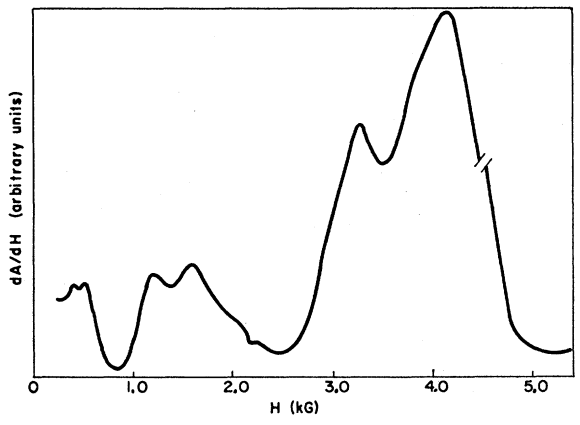


FIG. 7. Experimental trace of $dA/dH$ versus $H$ for the Voigt configuration with **H**∥⟨110⟩.

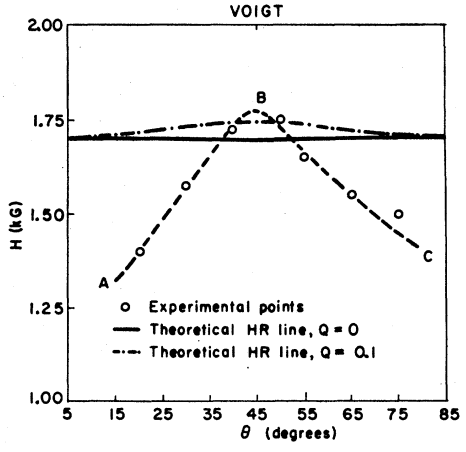


FIG. 8. Comparison of the experimental curve ABC and theoretical curves for the hybrid resonance.

0.1%. Therefore, although the data are not complete enough to permit a calculation of $\epsilon_L$, the position of the peak of curve ABC does appear to indicate that $\epsilon_L > 400$.

Still to be explained is the large dropoff with angle of curve ABC, which is in radical disagreement with the predicted variation of the position of the HR in the Voigt geometry for any value of $Q$. This behavior results from the mixing in of the Faraday mode as **H** is rotated away from $\theta = 45°$. The analysis of the resulting angular behavior of the HR line is difficult if full mass anisotropy is included, but has been carried out for a simplified model which replaces the ellipsoids with spheres of the appropriate masses. The result, valid only for small angles $\delta = \theta - 45°$, is

$$\Delta \equiv \frac{H(\delta)-H(0)}{H(0)} = -\frac{1}{8}\left(\frac{r^2-1}{r}\right)^2 \delta^2 \equiv -B\delta^2, \quad (25)$$

where $H(\delta)$ is the position of the HR at the angle $\delta$ and $r = \omega_{ca}/\omega_{cb}$. From the measured values of the parameters, $r = 2.6$ and $B = 0.6$. A quadratic least-squares fit of the experimental values of $\Delta$ versus $\delta$, of the form $\Delta = -C_1\delta^2 + C_2\delta + C_3$, gives $C_1 = 0.6 \gg C_2, C_3$. Therefore, curve ABC conforms in both position and shape to the HR line as it appears in the mixed Voigt-Faraday geometry, and this agreement is dependent upon the choice of the 1.3-kG line as the OR. The measured positions of the ER, the OR, the HR, and the Azbel-Kaner subharmonics are thus internally consistent for $K = 9.7$ and $m_t/m_0 = 0.043$.

With the values of $K$ and $m_t$ fixed, the dielectric-anomaly data can be used to calculate $\epsilon_L$. Again, to ensure that no Doppler effects enter, the data at $\theta = 45°$ are used. At this angle, the high-field extraordinary-mode dielectric anomaly (EDA) occurs at 4.65 kG, and the low-field EDA at 2.20 kG. The position of the latter is too insensitive to the value of $\epsilon_L/n$ to allow a calculation. Using only the high-field result, a computer analysis of $\eta_e^2\langle 110\rangle$ indicates that $\epsilon_L/n$ lies in the range $(0.3\text{–}2.2)\times 10^{-14}$, with a central value of $1.4\times 10^{-14}$. The spread in these values derives from the uncertainties in the mass parameters and the magnetic field measurement. Using the Hall value for $n$, the lattice dielectric constant is calculated to lie in the range $2.4\times 10^3$–$1.8\times 10^4$, with a central value of $1.2\times 10^4$. Though there is a very large uncertainty in these values , it is significant that even the lower limit is six times as large as the accepted value. The theoretical dielectric-anomaly curves in Fig. 6 use the central value of $\epsilon_L/n$ and are seen to fit the data closely near $\theta = 45°$.

The dashed low-field lines in Fig. 6 are drawn as the first and second subharmonics of the OR curve and are seen to be a good fit to the data for all values of $\theta$. The fit can be quantitatively verified by plotting $H_p$, the field at which the $(p-1)$th subharmonic occurs, against $1/p$, $p = 1, 2, 3, \cdots$. This plot should give a straight line passing through the origin with slope $m^*\omega c/e$, where $m^*$ is the cyclotron mass for the primary resonance, the OR. A least-squares line fitted to the data does pass through the origin, and the mass calculated from the slope is $0.055\ m_0$. The mass corresponding to the OR curve, using the measured values of $K$ and $m_t$ and averaging over $\theta$, is $0.058\ m_0$. The two mass values agree to within 5% and the low-field points lie accurately at the positions of the Azbel-Kaner subharmonics. These low-field resonances appeared as very small peaks in the $dA/dH$ traces, and it is not surprising that the much weaker subharmonics of the ER do not appear.

Figure 6 also exhibits some features which may be Doppler effects. The local theory predicts that, with the exceptions of the HR and ODA, every resonance and dielectric anomaly which appears at $\theta = 45°$ should also appear, at the same magnetic field, at $\theta = 135°$. The data do not bear out this prediction; every peak at 135° is shifted relative to the corresponding peak at 45°, with the magnitudes of the shifts ranging from 4 to 19%. Except for the fact that the 1.3-kG line seems to have split both up and down, all the shifts are to higher magnetic fields, as they should be if they are Doppler shifts.

The observed shifts are generally too large to be ascribed to either changes in the klystron frequency or sample misalignment errors. The klystron frequency was held constant to better than 1% by cavity tuning and an AFC system, while the accumulated misalignment errors could account for shifts of 5% at most.

The observed shifts can be compared to the theoretical values obtained by the Doppler parabola method, since all the parameters necessary for the calculation have been obtained from the local data. The comparison is made in Table I, where both $\eta_+^2\langle 110\rangle$ and $\eta_-^2\langle 110\rangle$ have been used. The upward shift in the 1.3-kG resonance and the shift in the 4.65-kG dielectric anomaly agree closely with the predicted values. The downward 17% shift in the 1.3-kG line is not predicted at all. The observed 4% shift in the 2.2-kG dielectric anomaly is also not predicted, and the theoretical values for the shift in the 3.4-kG resonance are too large for either mode.

TABLE I. Comparison of observed shifts in the Faraday configuration with calculated Doppler shifts. R = resonance; DA = dielectric anomaly.

| Effect and mode | Predicted position Local theory (kG) | Observed shift (%) | Calculated Doppler shift (+) Mode (%) | (−) Mode (%) |
|---|---|---|---|---|
| R + | 1.28 | 19 | 18 | 0 |
| | | −17 | 0 | 0 |
| DA + | 2.20 | 4 | 0 | 0 |
| R ± | 3.38 | 4 | 17 | 8 |
| DA − | 4.65 | 10 | 11 | 0 |

## 6. CONCLUSIONS

The present local results for $n$-type PbTe are consistent with the $\langle 111\rangle$-ellipsoid model, and yield $K=9.7$ and $m_t/m_0=0.043$ at a concentration of $8.1\times10^{17}$ cm$^{-3}$. All the local magnetoplasma effects predicted from this model were obtained, except that, in the vicinity of 1.3 kG, where two closely spaced lines should have appeared, only one was observed. This line was taken to be the ordinary-mode cyclotron resonance, because this interpretation led to consistent results for the positions of the HR and the two Azbel-Kaner subharmonics. Nii, in his results for $n$-PbTe at 70 GHz, also observed only one line, but interpreted it as due to the ODA. His data analysis based on this interpretation gave $K=10$ and $m_t/m_0=0.024$ at a concentration of $1.9\times10^{17}$ cm$^{-3}$. Because Nii observed only one Azbel-Kaner subharmonic and did not see the HR at all, it was not possible for him to check his interpretation as fully as has been done here.

Two Azbel-Kaner subharmonics have been observed. In metals, the nonlocal parameter $qv_F/\omega_c$ is of the order of several hundred, and $qv_F/\omega_c\gg1$ is usually taken as the condition for the Azbel-Kaner effect. The present results show that the Azbel-Kaner resonances, though weak, are observable for $qv_F/\omega_c<1$. The appearance of two subharmonics lends weight to the suggestion of Nii that the nearly isotropic light mass reported by Stiles *et al.*[3] was in reality the first subharmonic of the ordinary resonance. The observed subharmonics arise from a tilted-orbit cyclotron resonance and carry through continuously as $\mathbf{H}$ is rotated from $\theta=45°$ to $\theta=135°$; thus, their behavior conforms to the prediction that, for a tilted ellipsoid, Azbel-Kaner cyclotron resonance occurs in both the Voigt and Faraday geometries. There is no evidence that the subharmonics themselves are Doppler-shifted in the Faraday geometry, but the shifts may be too small to be easily observed.

Of the five shifts in position for the resonances and dielectric anomalies observed in the Faraday geometry, two agree with the predictions from the Doppler parabola method. The downward shift in the 1.3-kG line to about 1.1 kG may represent the secondary Doppler peak discussed by Miller and Haering,[2] which does not appear in the present theory because the simplification $\omega\tau\rightarrow\infty$ has been made. This lower line appears as if it might be a continuation of the HR curve ABC. It would be of interest to determine how the HR relates to the Doppler-shifted cyclotron resonances as $\theta$ approaches 135°, but the required theory would be very complex, since it would have to include the general mixed Voigt-Faraday geometry and mass anisotropy, as well as nonlocal terms. The analysis of all these effects is greatly complicated because of the lack of single mode excitation in the {110} sample. A more definite determination could be made by applying circularly polarized radiation to a {100} sample and studying the behavior of the resonance as a function of frequency; this approach was used by Kirsch[18] in his investigation of Doppler-shifted cyclotron resonance in Bi. The magnitudes of the Doppler shifts would be increased by working at frequencies below 70 GHz, but very high mobility samples would be needed to provide an adequate value for $\omega\tau$.

The result $\epsilon_L=1.2\times10^4$ was obtained by analysis of the dielectric-anomaly data, and the measured position of the HR is consistent with a value of this order of magnitude. The static dielectric constant $\epsilon_s$ may be calculated from $\epsilon_L$ and the known values of the high-frequency dielectric constant and longitudinal-optical frequency in PbTe; the result is $\epsilon_s=1\times10^4$. This value agrees with that obtained by Sawada *et al.*[7] in their high-magnetic-field helicon experiments on a $p$-type sample with concentration $5\times10^{17}$ cm$^{-3}$. Moreover, low-field helicon experiments carried out on the sample used in the present work also gave $\epsilon_s=1\times10^4$; these helicon experiments will be described in detail elsewhere. The discrepancy between these results and the value of 400 obtained in the previously cited experiments[8–11] is not understood, but it may be significant that the anomalously large values occur only in experiments where a magnetic field is applied to the sample.

## ACKNOWLEDGMENTS

The author would like to thank Professor E. Burstein for his sponsorship of this thesis work and is grateful to Dr. R. Rediker and Dr. A. R. Calawa of the MIT Lincoln Laboratory for supplying samples. The author also wishes to thank General Telephone and Electronics Laboratories, Inc., Bayside, N. Y., for providing facilities for the preparation of this manuscript.

[18] J. Kirsch, Phys. Rev. **133**, A1390 (1964).